



**HAL**  
open science

# Laboratory methods for testing the performance of acoustic rail dampers

Martin Toward, David Thompson

► **To cite this version:**

Martin Toward, David Thompson. Laboratory methods for testing the performance of acoustic rail dampers. Acoustics 2012, Apr 2012, Nantes, France. hal-00810837

**HAL Id: hal-00810837**

**<https://hal.science/hal-00810837>**

Submitted on 23 Apr 2012

**HAL** is a multi-disciplinary open access archive for the deposit and dissemination of scientific research documents, whether they are published or not. The documents may come from teaching and research institutions in France or abroad, or from public or private research centers.

L'archive ouverte pluridisciplinaire **HAL**, est destinée au dépôt et à la diffusion de documents scientifiques de niveau recherche, publiés ou non, émanant des établissements d'enseignement et de recherche français ou étrangers, des laboratoires publics ou privés.



# ACOUSTICS 2012

## Laboratory methods for testing the performance of acoustic rail dampers

M. Toward<sup>a</sup> and D. J. Thompson<sup>b</sup>

<sup>a</sup>Consultancy Group-ISVR - University of Southampton, University Road, SO17 1BJ  
Southampton, UK

<sup>b</sup>Dynamics Group-ISVR - University of Southampton, University Road, SO17 1BJ  
Southampton, UK  
mgrt@soton.ac.uk

Rail dampers are now commercially available to reduce noise radiated by railway track by increasing the attenuation with distance of vibration transmitted along the rail (decay rate). These dampers, attached to the rail between sleepers, work on the principle of a tuned mass-spring absorber. Currently, there are no standardized procedures to measure the effectiveness of these dampers without the need for their installation in a track. Here, decay rates of damped 'freely supported' rails have been measured using two proposed methods: (i) for long rails, by integrating decay rates derived from FRF's measured at intervals along the rail; and (ii) for short rails, at low frequency from the modal properties of the rail, and at high frequencies directly from point and transfer responses functions (FRFs) at either end of the rail. The two methods show reasonable agreement in vertical and lateral decay rates between 300 Hz and 5 kHz. Further tests on a 32m test track show that decay rates of damped track can be determined reasonably well by summing the decay rates of the 'free' damped rail and the decay rates of the undamped track. Systematic variations in decay rates were found with rail pad and damper temperature.

## 1 Introduction

In most situations, noise originating from the interaction of the wheel and rail (i.e. rolling noise) is the dominant source of environmental railway noise. In Figure 1, it can be seen that, while the sleeper is generally the major noise source below 400 Hz and the wheel is of increasing importance above 1600 Hz, between 500 Hz and 2 kHz (and overall), noise radiated from the rail is the dominant source. Increasing the stiffness of the rail pads between the rail and sleeper can decrease the rail component of rolling noise but conversely increase the noise radiated from the sleeper due to the increased coupling. In practice soft pads (<250 MN/m) tend to be used to reduce damage to the ballast and sleepers, although they are not optimal for noise.

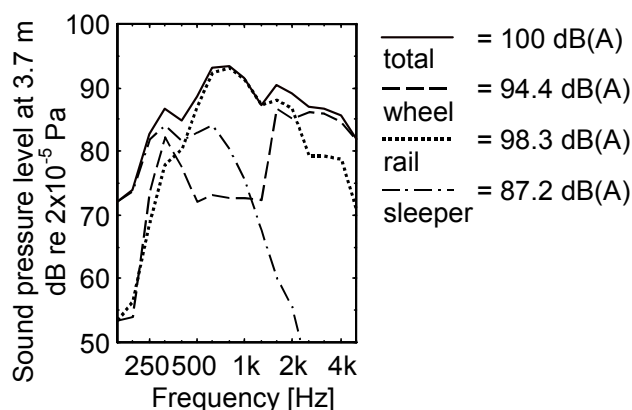


Figure 1: Example predictions from TWINS model showing contributions to total noise (from [1])

Rail dampers are designed to reduce rail noise by increasing the attenuation with distance of the rail (decay rate) and hence reducing the radiating length. Several designs of damper are now commercially available. Generally, these dampers are bolted or clipped on to the rail between sleepers and claim to work on the principle of tuned mass dampers. Overall noise level reductions of 2 to 6 dB(A) have been shown in comparative measurements of dampers installed within a track [2-4], with reductions greatest with softer rail pads [4] and when the rail roughness is high [3]. However, currently, there are no standardized procedures to test the performance of rail dampers.

An objective of the Franco-German STARDAMP project is to define methodologies to test rail dampers in the laboratory without the need for their installation in a track, with the attendant cost, time and variability implications.

To these ends, two methods have been proposed to measure the decay rates of damped 'freely supported' rails.

## 2 Methodology

Results are presented from laboratory tests according to two proposed methods, for 'short' and 'long' rails. The premise of both methods is that the decay rates of a damped track can be found from summing the decay rates of a damped 'freely supported' rail and the decay rates of an undamped track. This is tested in Section 3.

Various types of damper have been tested but the results given here relate to Schrey and Veit rail dampers shown in Figure 2. These dampers consist of two 7.0 kg laminated rubber and steel construction absorber masses bolted on to the rail web via a solid steel base plate (2.8 kg). The total mass of each damper assembly is 18.6 kg.



Figure 2: Schrey and Veit rail damper

### 2.1 Long rail method

Measurements were conducted on a 32 m test track at the University of Southampton. The track was designed to be broadly representative of circulated track within the UK: UIC 60 rail, 51 concrete monobloc sleepers spaced nominally at 0.6 m (0.54 - 0.8 m), Pandrol fastclips, Pandrol 10 mm studded natural rubber pads (effective stiffness approx. 120 MN/m) and granite ballast to a depth of 0.3 m.

Measurements were made of the decay rates of the undamped track, the damped track and the damped 'freely supported' rail. In each case vertical and lateral decay rates were measured using a method based on that described in EN 15461:2008 [5]. A measurement grid was marked up from a reference point 10 sleeper spans (5.96 m) from the rail end. Measurements were made at 1/4-sleeper intervals from this point up to the 16<sup>th</sup> sleeper span, then at mid-span positions 17, 18, 20, 22, 26, 30, 34, 38, 42 and 46.

An ICP accelerometer was attached using a thin layer of beeswax at the reference point, either at the centre of the rail head for vertical measurements or on the side of the rail head for lateral measurements. A 160g ICP instrumented hammer, with a titanium tip, was used to excite the rail. The force spectrum was approximately flat up to 7 kHz (within 20 dB).

Decay rates,  $DR$ s, in each  $\frac{1}{3}$  octave band up to 5 kHz were calculated in dB/m from [5]:

$$DR = \frac{4.343}{\sum_{x=0}^{x_{\max}} \frac{|A(x_n)|^2}{|A(x_0)|^2} \Delta x_n} \quad (1)$$

where,  $A(x_0)$  and  $A(x_n)$  are the point and transfer frequency-response functions (FRFs) respectively in each  $\frac{1}{3}$  octave band, and  $x_n$  is the measurement position.

The point FRF was derived for excitation at a position 20 mm grid-side of the accelerometer, averaged over  $\geq 10$  impacts. Transfer FRFs were derived from excitation at each of the grid positions using  $\geq 4$  impacts. Data was acquired at a rate of 25 k samples/sec (10 kHz bandwidth) with no windowing. The acquisition duration was 320 ms (including 10 ms force pre-trigger) resulting in a frequency resolution of 3.1 Hz. Mobility FRFs (i.e. velocity over force) were used throughout the analysis.

For the damped conditions, the dampers were bolted on at mid span along the full length of the rail, except at inter-sleeper positions 18 and 37 where rail welds prevented their attachment. For the damped ‘free-rail’ condition, the rail was unclipped and supported on sections of hydraulic hose resulting in a bounce mode of the rail at  $\approx 15$  Hz. This was measured with the impact hammer fitted with a soft tip. Rail temperatures were measured at the start and end of each measurement-set using a thermocouple attached to the underside of the rail; average temperatures are reported.

## 2.2 Short rail method

At low frequencies, decay rates were derived from the modal properties of the rail and at high frequencies, where the modal damping was high, by directly measuring the attenuation along the length of the rail [2]. Unless mentioned otherwise, details of instrumentation and analysis were common with the long-rail method.

Ten dampers were installed at 0.6 m intervals over a 6 m length of UIC 60 rail (i.e. 10 in total). The rail was supported at either end on stacks of 12 rubber rail-pads, resulting in a bounce mode of  $\approx 20$  Hz. Miniature ICP accelerometers were mounted as close as possible to either end of the rail (i.e. 5 mm). For both lateral and vertical measurements, a point FRF at one end and a transfer FRF to the other end was measured. Additionally, the transfer FRF to the mid-rail position was added to assist modal identification. Measurements were conducted in a heated ( $20 \pm 2$  °C) laboratory.

At low frequency, typically below 500 Hz, where distinct peaks in the FRFs could be observed, decay rates for each mode were derived from the point FRF using:

$$DR = 4.343 \frac{\omega \eta}{c_g} \quad (2)$$

where, the resonance frequency,  $\omega$ , and the modal loss factor,  $\eta$ , were found using a circle fitting technique implemented in MATLAB, e.g. see [6]. To determine the group velocity,  $c_g$ , first, the wavenumber of each mode was calculated from the order of the mode,  $n$ , and the rail length,  $L$ :

$$k_n = (n + \frac{1}{2})\pi/L, \text{ for } n = 1,2,3,\dots \quad (3)$$

Then, the dispersion curve (wavenumber versus modal frequency) for the rail was plotted, and finally the group velocity was estimated as the slope of the dispersion curve. The gradient at each resonance frequency was calculated as the average of the slopes on either side of this frequency, thus decay rates were not calculated for the first and last identified modes. Further details of this method can be found in [2].

At high frequency, typically above 400 Hz, the decay rates were determined directly from the ratio of the transfer FRF to the point FRF, each expressed in  $\frac{1}{3}$  octave bands. The lower frequency limit of this method was determined as the subsequent  $\frac{1}{3}$  octave band to the highest band with a negative calculated decay rate.

## 3 Results and discussion

### 3.1 Long rail results

Measured vertical decay rates for the undamped track, the damped ‘freely supported’ rail and the damped track are shown in Figure 3. For the undamped track, at low frequencies, there is high attenuation because of the stiffness of the foundation. At around 250 Hz there is a broad peak associated with the sleeper and pad acting as a ‘dynamic absorber’. Above around 500 Hz, waves begin to propagate freely in the rail and the decay rate decreases, before increasing again to a peak at around 5 kHz, caused by a flapping mode of the rail foot [1]. This broad dip in the vertical decay rates coincides with the peak in the noise spectrum illustrated in Figure 1 and therefore an effective damper will increase damping and thus reduce noise in this region. Measurements in the lateral direction showed similar trends (Figure 4). One difference was that the undamped lateral track decay rates were, at most frequencies, at a much lower level than in the vertical direction. The lower lateral rates explain why, while the excitation is generally lower in the lateral direction, its contribution to overall noise levels can be of significance.

The damped ‘free’ rail decay rates in both directions (Figures 3 and 4) show that the dampers introduced high decay rates in the region of the trough in the undamped track decay rates. Evidence of several broad peaks (e.g. 500, 1000, 2500 Hz in the vertical direction) is consistent with the multi degree-of-freedom design of the damper.

Damped track decay rates have been predicted by summing the damped ‘free’ rail decay rates with those of the undamped track (Figures 3 and 4). These show reasonable agreement with the directly measured decay rates at most frequencies. Some explanations for inaccuracies in the predicted decay rates are discussed later.

The expected reduction in noise from the rail in each  $\frac{1}{3}$  octave band, from installing dampers,  $\Delta L$ , can be calculated from the undamped track decay rate,  $DR_u$  and the damped track decay rate,  $DR_d$  according to:

$$\Delta L = 10 \log_{10} \frac{DR_u}{DR_d} \quad (4)$$

This implies that the maximum improvement in the vertical rail component of rolling noise would be 14.4 dB at 2 kHz, and in the lateral direction would be 15.5 dB at 1 kHz. To calculate improvements to the overall sound level, predictions would be required of the contribution of the individual track components (e.g. Figure 1), including predictions of the 'typical' excitation spectra, e.g. using TWINS [1].

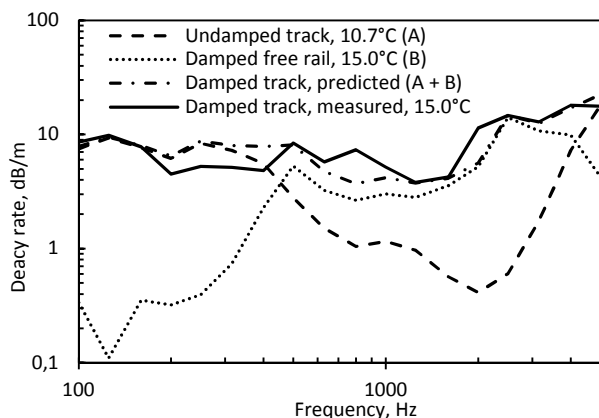


Figure 3: Vertical decay rates measured on the 32 m test track.

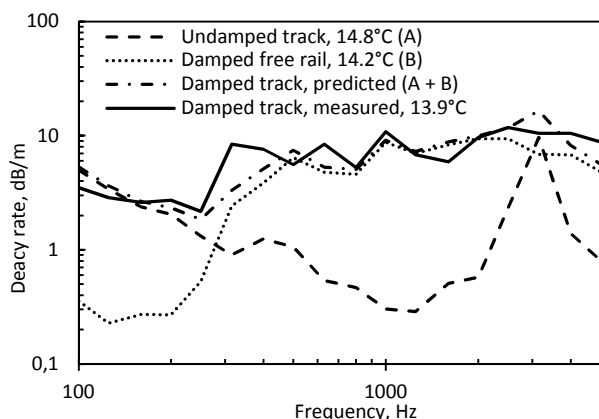


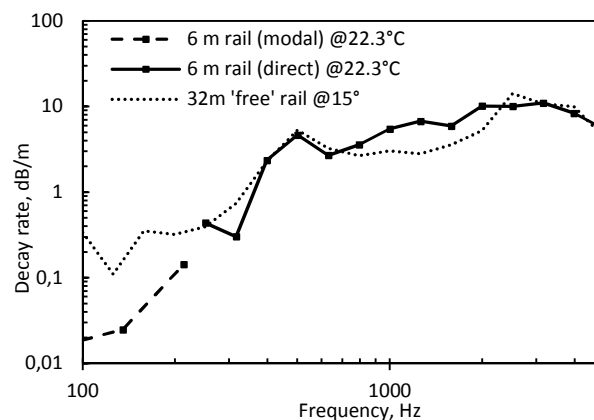
Figure 4: Lateral decay rates measured on the 32 m test track.

### 3.2 Short rail results

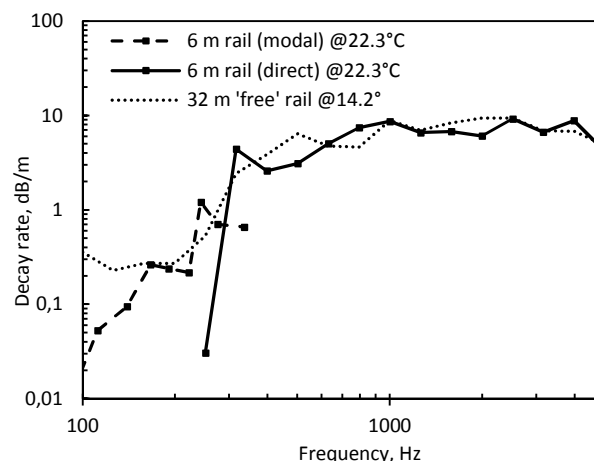
Vertical and lateral decay rates calculated according to the short-rail method are given in Figures 5 and 6 respectively. In these plots, the decay rates derived from the modal method and the direct method are compared with the decay rates of the damped 'free' rail measured using the long-rail method.

In the vertical direction, the highest clearly identifiable mode was at 301 Hz. However, as the group velocity was calculated from the dispersion curve (see Section 2.2 and Figure 7), the maximum frequency to which the decay rate could be calculated was the mode below this, i.e. 214 Hz. Likewise the group velocity could not be estimated for the lowest frequency mode, i.e. 26 Hz. In effect, using this method, the vertical decay rates could only be calculated at

three frequencies. Furthermore, the decay rates calculated at these frequencies were much lower than those measured from the long-rail method. This may be due to limitations of the long-rail method at low decay rates but in any case these small values are much smaller than the values applying in track (Figures 3 and 4).



Figures 5: Vertical decay rates measured on the 6 m rail compared to the 'freely supported' damped 32 m rail.



Figures 6: Lateral decay rates measured on the 6 m rail compared to the 'freely supported' damped 32 m rail.

In the lateral direction, decay rates could be calculated at a greater number of modal frequencies (ten modes between 56 Hz and 336 Hz). However, the lateral dispersion curve (Figure 7), exhibits a number of disparities i.e., the irregular result at around 95 Hz and the downward slope of the last two points. Timoshenko beam theory predicts that, at low frequencies, the dispersion curve should be linear (when plotted on a log-log scale), and that at higher frequencies, the slope should curve upwards as shear deformation becomes important [2]. A possible explanation for these differences might be that internal modes or mounting modes of the dampers interfered with the rail modes. Nevertheless, decay rates measured using the modal method in the lateral direction showed generally better agreement with the long rail measurements than was the case in the vertical direction.

Previous measurements have shown that vertical and lateral decay rates of a damped 4 m rail can be calculated up to at least 1 kHz using this modal method [2]. The reason for the higher frequency limit in the previous study might simply be that the damper decay rates in that study

were lower, particularly at low frequencies, resulting in the modal peaks being identifiable to higher frequencies.

Above 300 Hz, vertical decay rates derived using the direct method on the 6 m rail agree quite well with those obtained on the 32 m rail. However, decay rates between 800 Hz and 2 kHz were somewhat higher for the 6 m rail than for the long rail with a maximum difference of 3.8 dB (at 1.25 kHz). In the lateral direction, the fit was generally better, but yet still with notable differences at some frequencies (e.g. 3.3 dB at 500 Hz). These differences might be associated with temperature effects on the dampers (see Section 3.3) but could also be associated with some other methodological differences, e.g. end effects of the rails due to their finite length.

Where decay rates are low (generally at low frequency) the uncertainty in the direct short-rail measurement method increases due to the similarity of the responses at either end of the rail; these measurement errors may account for some of the differences between the 6 m and 32 m rail decay rates below 400 Hz (e.g. 250 Hz in Figure 5). The results suggest that for a 6 m rail, a lower ‘limit’ of reliable decay rates from the short rail method might be in the region of 1 dB/m. Increasing the rail length beyond 6 m is likely to lower this ‘limit’. However, given that the track decay rates are much higher than the damper decay rates below 400 Hz in most situations, the damper contribution to the track decay rate at these frequencies is in any case likely to be negligible.

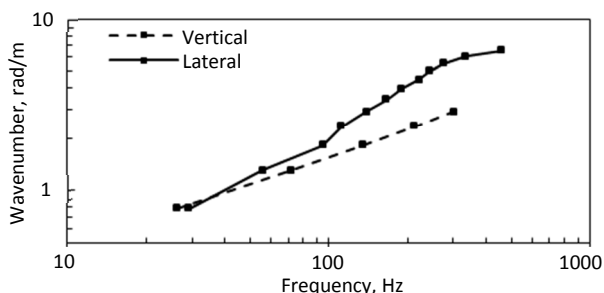


Figure 7: Dispersion curves for 6 m rail with dampers fitted.

### 3.3 Measurement variability

Figure 8 shows the temperature dependence of the decay rates of both the rails of the undamped 32 m track in the vertical direction. With both rails, the decay rates consistently decrease between 300 Hz and 2 kHz with each increase in temperature. It is likely that the temperature dependency of the rail pads was largely responsible for these effects, with any temperature effects on the track foundation expected to be restricted to low frequencies. These results suggest that increasing temperature is consistent with decreasing pad stiffness, i.e. decreasing the frequency of the sleeper-pad resonance at around 250 Hz [7,8]. Temperature dependence in the lateral direction shows similar, though less pronounced, trends (Figure 9).

Interestingly, in both directions there were also substantial variations in the decay rates between the two rails even at the same temperature (compare the solid line and the marked dotted line in Figures 8), even though the track structure was nominally the same under the two rails. One possible explanation for this is that while the east rail had been unclipped and reclipped prior to making the measurement, the west rail had not been unclipped for at

least 12 months previously. Again, the implication is that there was a reduction in pad stiffness caused by the process of unclipping and reclipping the rail.

These findings suggest that where possible, track measurements should be conducted over a narrow temperature range in order to improve damped track decay rate predictions. An alternative approach might be to model these temperature effects and account for any differences from a ‘standardized’ condition by corrections to the measurements. Further experimental measurements of the temperature and time dependence of rail pads would aid to improve the accuracy of such a model.

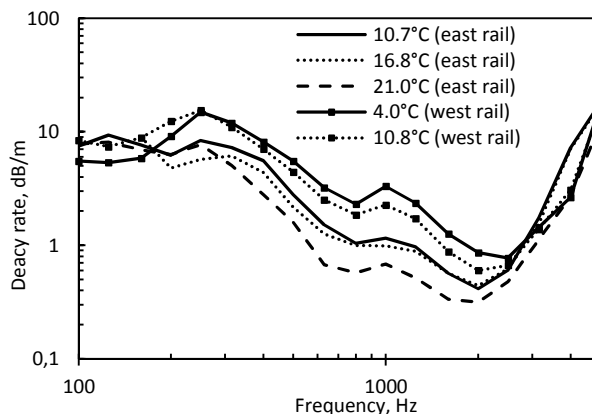


Figure 8: Effects of rail temperature and rail on vertical decay rates of the undamped 32 m track.

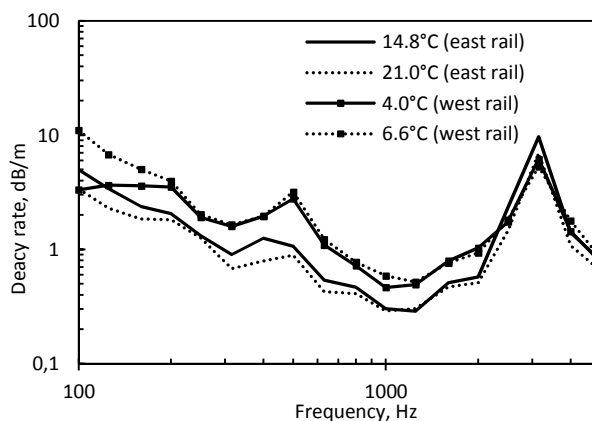


Figure 9: Effects of rail temperature and rail on lateral decay rates of the 32 m undamped track.

Figure 10 shows the effects of temperature on the decay rates of the damped ‘freely supported’ rail. Assuming no effect of temperature on the rail itself, this suggests that the rail-damper material properties were affected. In both directions, at frequencies above 1.6 kHz the decay rates decreased with increasing rail temperature, while from 250 to 500 Hz the rates increased with increasing temperature; inconsistent effects were found at other frequencies. While it would be expected that equivalent effects would be evident with other damper designs, their nature is likely to depend to a great extent on the design of the specific damper. Consequently, although the effects of temperature on a much simpler damper design have previously been modelled and corrected for in the prediction of decay rates, it is unlikely to be a feasible approach in a universal test method [2]. For this reason controlling the test environment is likely to be a more practicable approach. This would tend to support the short rail test method, being easier to facilitate in a controlled environment (i.e. indoors).

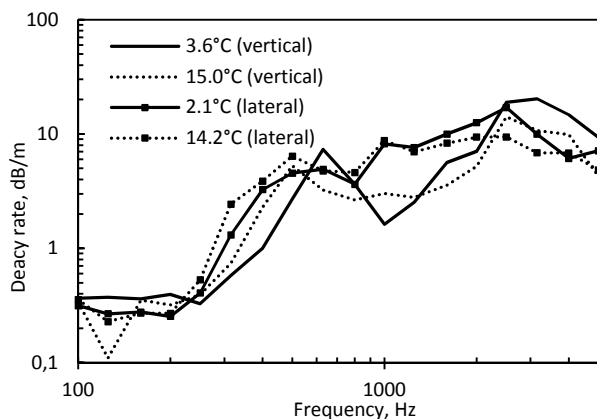


Figure 10: Effects of rail temperature on decay rates of the damped 'freely supported' 32 m rail.

## 5 Conclusions

The two methods for determining decay rates of damped 'freely supported' rails show reasonable agreement between 300 Hz and 5 kHz. The modal method for determining decay rates on the 'short' 6 m rail was restricted to low frequencies (< 300 Hz) and resulted in much lower rates than those measured on the 'long' 32 m rail. As the damper decay rates are relatively low below 400 Hz and tend to have little influence on overall track decay rates, the direct short-rail method, yielding plausible measurements down to 300 Hz, may be sufficient for many applications.

In the vertical direction, between 800 Hz and 2 kHz, the 'direct' short rail method resulted in higher decay rates than for the long rail method. While the temperature dependence of the damper may have contributed to these differences, other causes cannot be discounted, e.g. end effects due to the finite rail lengths. Measuring the 'free' rail in a controlled environment would remove the effects of temperature, tending to favour the short rail test method for reasons of practicality. Modelling of the transmission of vibration in the rail could help to establish the presence and influence of end effects.

Vertical and lateral decay rates of a damped 32 m track predicted from the decay rates of the undamped track and the 32 m 'freely supported' rail agreed quite well with measurements of the damped track. However, there were differences at some frequencies. Both increasing rail pad temperature and unclipping/reclipping the rail reduced decay rates between 300 Hz and 2 kHz – the accuracy of predictions could be improved if these effects are controlled or at least accounted for in measurements.

Further work is required to gain greater understanding of the effects of temperature on the track components, particularly the rail pad, and rail dampers. Nevertheless the proposed laboratory test method appears to be suitable to form a standardized method for assessing different rail dampers.

## Acknowledgments

The authors would like to acknowledge the assistance of the STARDAMP partners: Alstom, Deutsche Bahn, GHH-Valdunes, SNCF, Schrey & Veit, Tata Steel, TU Berlin and Vibratex and the funding from the Deufrako cooperation (German funding by BMWI; FKZ 19U10012 A, B, C, D); French funding by FUI).

## References

- [1] D.J. Thompson, *Railway Noise and Vibration: Mechanisms Modelling and Means of Control*, Elsevier (2009)
- [2] D.J. Thompson, C.J.C Jones, T.P. Waters, D. Farrington, "A tuned damping device for reducing noise from railway track", *Appl. Acoust.* 68, 43-57 (2007)
- [3] E. van Haaren, G. A. van Keulen, "New Rail Dampers at the Railway Link Roosendaal-Vlissingen Tested within the Dutch Innovation Program" *Notes on Numerical Fluid Mechanics and Multidisciplinary Design*, 99, 378-83 (2008)
- [4] B. Asmussen, D. Stiebel, P. Kitson, D. Farrington, D. Benton, "Reducing the Noise Emission by Increasing the Damping of the Rail: Results of a Field Test", *Notes on Numerical Fluid Mechanics and Multidisciplinary Design*, 99, 229-35 (2008)
- [5] CEN. Railway applications – Noise emissions, "Characterization of the dynamic properties of track sections for pass by noise measurements, EN 15461 (2008)
- [6] D.J. Ewins, *Modal Testing: Theory, Practice and Application*, Wiley-Blackwell (2000)
- [7] D.J. Thompson, C.J.C Jones, T.X. Wu and G. de France. "The influence of the non-linear behaviour of railpads on the track component of rail noise" *Proceedings of the Institution of Mechanical Engineers*, Part F, 213, 233-241, 1999.
- [8] R.A. Broadbent, D.J. Thompson and C.J.C. Jones, "Evaluation of the effects of temperature on railpad properties, rail decay rates and noise radiation", *Proceedings of 16<sup>th</sup> International Congress on Sound and Vibration*, Krakow, July 2009.